Clinical and Translational Radiation Oncology 39 (2023) 100577

Contents lists available at ScienceDirect

Clinical and Translational Radiation Oncology

journal homepage: www.sciencedirect.com/journal/clinical-and-translational-radiation-oncology

First treatments for Lattice stereotactic body radiation therapy using magnetic resonance image guided radiation therapy

Alex T. Price [a,*], Joshua P. Schiff [b], Tong Zhu [b], Thomas Mazur [b], James A. Kavanaugh [c], Borna Maraghechi [b], Olga Green [d], Hyun Kim [b], Matthew B. Spraker [e], Lauren E. Henke [a]

[a] Department of Radiation Oncology, University Hospitals, Cleveland, OH, USA
[b] Department of Radiation Oncology, Washington University in St Louis School of Medicine, St. Louis, MO, USA
[c] Department of Radiation Oncology, Mayo Clinic, Rochester, MN, USA
[d] Varian Medical Systems, Inc., Palo Alto, CA, USA
[e] Centura Health, Denver, CO, USA

ARTICLE INFO

Keywords
Lattice
SBRT
MRgRT
Image features

ABSTRACT

Two abdominal patients were treated with Lattice stereotactic body radiation therapy (SBRT) using magnetic resonance guided radiation therapy (MRgRT). This is one of the first reported treatments of Lattice SBRT with the use of MRgRT. A description of the treatment approach and planning considerations were incorporated into this report. MRgRT Lattice SBRT delivered similar planning quality metrics to established dosimetric parameters for Lattice SBRT. Increased signal intensity were seen in the MRI treatments for one of the patients during the course of treatment.

Introduction

Spatially fractionated radiation therapy (SFRT) delivers an intentional and often times patterned non-uniform target doses to bulky locally advanced tumors[1,2]. Such techniques have shown promise in soft-tissue sarcomas previously and has led to the development and international recommendations for further prospective clinical trials in a variety of disease sites[2,3]. Lattice stereotactic body radiation therapy (SBRT) is a recently developed SFRT technique that delivers 2000 cGy in 5 fractions to tumor volumes with a 6670 cGy simultaneous integrated boost in a lattice-type geometric pattern[4].

Magnetic resonance image-guided radiation therapy (MRgRT) provides improved soft-tissue contrast for patient alignment compared to traditional cone-beam computed tomography (CBCT) guided techniques [5]. Additionally, real-time cine MRI for motion monitoring can support gated treatment based directly on measured target motion, thus enabling reduced target volumes without compromising accuracy or precision[6,7].

Here we present 2 MRI-guided Lattice SBRT cases in the abdomen treated using the ViewRay MRIdian platform (ViewRay, Inc, Cleveland, OH, USA) where MRgRT provided excellent alignment based on soft tissue and real-time motion monitoring.

Treatment planning and delivery

Patients received MRgRT treatment because both targets were located within the liver, with lesions being difficult to visualize on CT imaging and no fiducial markers being present to support CBCT-based localization. The patients also had relevant organs at risk (OARs) in close proximity, which underscored the importance of soft tissue visualization using MRI guidance when aligning the patient to avoid unsafe doses to these OARs.

Both patients received a CT simulation and ViewRay 0.35T MRI simulation with both arms up in a foam-based immobilization system. During CT simulation, a 4D-CT and an end-exhale breath-hold image were acquired. During the ViewRay simulation, both an end-exhale breath-hold volumetric image (17 s) and a two-dimensional free-breathing cine image were acquired to assess tumor visualization and tracking ability on the ViewRay system. The end-exhale breath-hold 0.35T image was used as the primary dataset to remove motion artifacts and improve image quality.

The identified lesions on the MRI were contoured as gross tumor volume (GTV_2000). A 0.5 cm isotropic expansion was used to create the planning target volume (PTV_2000). A geometrical arrangement of high dose 1.5 cm diameter spheres were placed within the GTV, as described

* Corresponding author.
E-mail address: alex.price@uhhospitals.org (A.T. Price).

https://doi.org/10.1016/j.ctro.2023.100577
Received 26 May 2022; Received in revised form 29 December 2022; Accepted 4 January 2023
Available online 6 January 2023

in a recently completed Phase I clinical trial[3]. These high dose spheres (PTV_6670) were treated as simultaneous-integrated boosts to 6670 cGy. A similar but offset arrangement of 1.5 cm PTV_Avoid spheres were placed to produce characteristic dose gradients between high-dose spheres. These PTV_Avoid structures were kept to a maximum dose of 1800 – 2000 cGy in 5 fractions. An additional PTV_2000_Opt structure was created, which was the PTV_2000 excluding the PTV_6670 + 1 cm isotropic margin and the PTV_Avoid. The PTV_2000_Opt structure was specifically made for the ViewRay planning system to remove conflicting objectives. A 1 cm ring structure surrounding the PTV_2000 vol was used in optimization to encourage 2000 cGy conformity and a skin rind structure was used to spread out relative dose contribution of all beams. Dosimetric and Lattice SBRT planning metrics are presented in Table 1. A 1.5 cm ring structure surrounding the PTV_6670 was created to assess dose gradients surrounding the high dose volumes.

At time of treatment, a 17 s end-exhale breath hold was acquired and registered to the 0.35T end-exhale breath-hold primary dataset. Once couch shifts were applied, a sagittal MR-cine image near the center of the target with clear contrasted boundaries between the target and surrounding tissue was acquired. Patients were treated at the end-exhale phase of their free-breathing cycle. Gating thresholds were evaluated on a per fraction basis. However, a maximum value of 1 % of the identified target (continuously deformed from the GTV structure defined on the alignment image) in the sagittal plane could be outside a gating boundary which was defined as a 3 mm smoothed expansion of GTV defined on the alignment image[8–10]. If the identified target exceeded 1 % outside the gating boundary, the beam would hold. Treatment delivery times were extracted for each fraction. The signal intensity changes within the PTV_6670 volumes relative to the PTV_Avoid volumes for the initial image and all subsequent fraction images were analyzed. The mean value of the pixels within the total structure, respectively, was extracted for this data.

Case 1

Presentation

A 50-year-old female initially presented with deep venous thrombosis. Approximately-one year later, her surveillance imaging demonstrated new hepatic lesions. Biopsy of one of the liver lesions confirmed a diagnosis of metastatic leiomyosarcoma. She subsequently proceeded to systemic therapy and over the next three years progressed on several lines of chemo- and targeted systemic therapies. She also underwent multiple local therapies including two courses of radiofrequency ablation to spinal metastases. She had no prior radiotherapy.

Most recently, she had received several months of Anlotinib on clinical study at a high-volume academic center. Surveillance systemic imaging included a CT chest/abdomen/pelvis with contrast which demonstrated progression of multiple hepatic masses in the right hemiliver, the largest of which was 5.0×4.5 cm in segment 8, as well as a progressive necrotic right inguinal mass measuring 3.0×3.2 cm. Her systemic therapy was discontinued due to progression and she was referred to radiation oncology for consideration of palliative radiotherapy. On presentation to radiation oncology, she endorsed worsening abdominal pain. She was recommended Lattice SBRT for durable palliation of her hepatic metastases on a phase II clinical trial (NCI 0553471).

Quantitative analysis

For planning, 29 beams (11 deg of separation) were placed to create a full pseudo-arc and resulting step-and-shoot plan included 79 segments. The duodenum, large bowel, stomach, liver, kidneys, and spinal cord were the relevant OARs for this case. All OAR planning objectives were met. Target coverage metrics included PTV_2000 V95%Rx = 99.1 % and the PTV_6670 V95%Rx = 99.7 %. All reported dosimetric and SFRT-specific indices are shown in Table 1. Isodose lines in three orthogonal planes intersecting the centroid of the GTV_2000 are shown in Fig. 1. The average total gated delivery time (initiation of beam delivery to final MU delivered) was 25.6 min (range: 20.9 min – 38.7 min). There were no treatment interruptions during delivery. There were noticeable signal intensity changes between PTV_6670 and PTV_Avoid volumes over the course of treatment ($R^2 = 0.73$), which is shown in Fig. 3.

Follow-up

At three months post-Lattice SRBT, the patient had surveillance imaging performed which demonstrated interval partial response to radiotherapy as indicated by decrease in size of treated lesions. The surveillance image was uploaded to the treatment planning software and the GTV was contoured, demonstrating a reduction in volume from 170.4 cc at time of simulation to 21.2 cc. She eventually progressed locally and regionally, and received an additional course of palliative Lattice SBRT to hepatic lesions approximately-one year later. Ultimately she progressed distantly and was subsequently lost to follow up.

Table 1
Dosimetric planning objectives used and benchmark metrics used for Lattice SBRT.

Serial Structure	Dose Max Objective	Reporting Metric	Case 1	Case 2	Median Reported (Kavanaugh et al.)
Large Bowel	3800 cGy	**GTV Size (cc)**	183.3	319.1	945
Small Bowel	3600 cGy	**Average Time (min)**	25.6	36.9	9.7
Stomach	3600 cGy	**Minimum Time (min)**	20.9	24.7	7.1
Heart	3800 cGy	**Maximum Time (min)**	38.7	50.5	23.4
Esophagus	3500 cGy	**Monitor Units**	5137.3	8184.3	3739
Duodenum	3600 cGy	**PTV_6670 Max (cGy)**	8114.0	8071.0	7610
Spinal Cord	2800 cGy	**PTV_6670 Mean (cGy)**	7439.0	7289.0	7180
Skin Rind	3850 cGy	**PTV_6670 V95%Rx (%)**	99.7	99.4	100.0
Parallel Structure	**Minimum Critical Volume Below Threhold**	**PTV_6670 Spheres (#)**	3.0	3.0	9
Kidney	1750 cGy at 200 cc	**PTV_2000 CI**	1.2	1.2	1.4
Liver	2100 cGy at 700 cc	**PTV_2000 V95%Rx (%)**	99.1	99.5	99.9
Target Structure	**Dose Coverage Objective**	**PTV_Avoid Mean (cGy)**	2156.0	2191.0	2100
PTV_2000	V95%Rx > 95.0 %	**PTV_Avoid V1800cGy (%)**	100.0	100.0	100.0
PTV_6670	V95%Rx > 95.0 %	**PTV_Avoid Max (cGy)**	2515.0	2615.0	3010
		1.5 cm Ring Dmean (cGy)	3212.0	3711.0	3620
		1.5 cm Ring Dmedian (cGy)	2820.0	3419.0	3350
		1.5 cm Ring Dstd-dev (cGy)	1098.0	1121.0	1100
		(1.5 cm Ring Dmedian)/(1.5 cm Ring Dstd-dev)	2.6	3.0	3.1
		(PTV_6670 Dmean)/(PTV_Avoid Dmean)	3.5	3.3	3.5

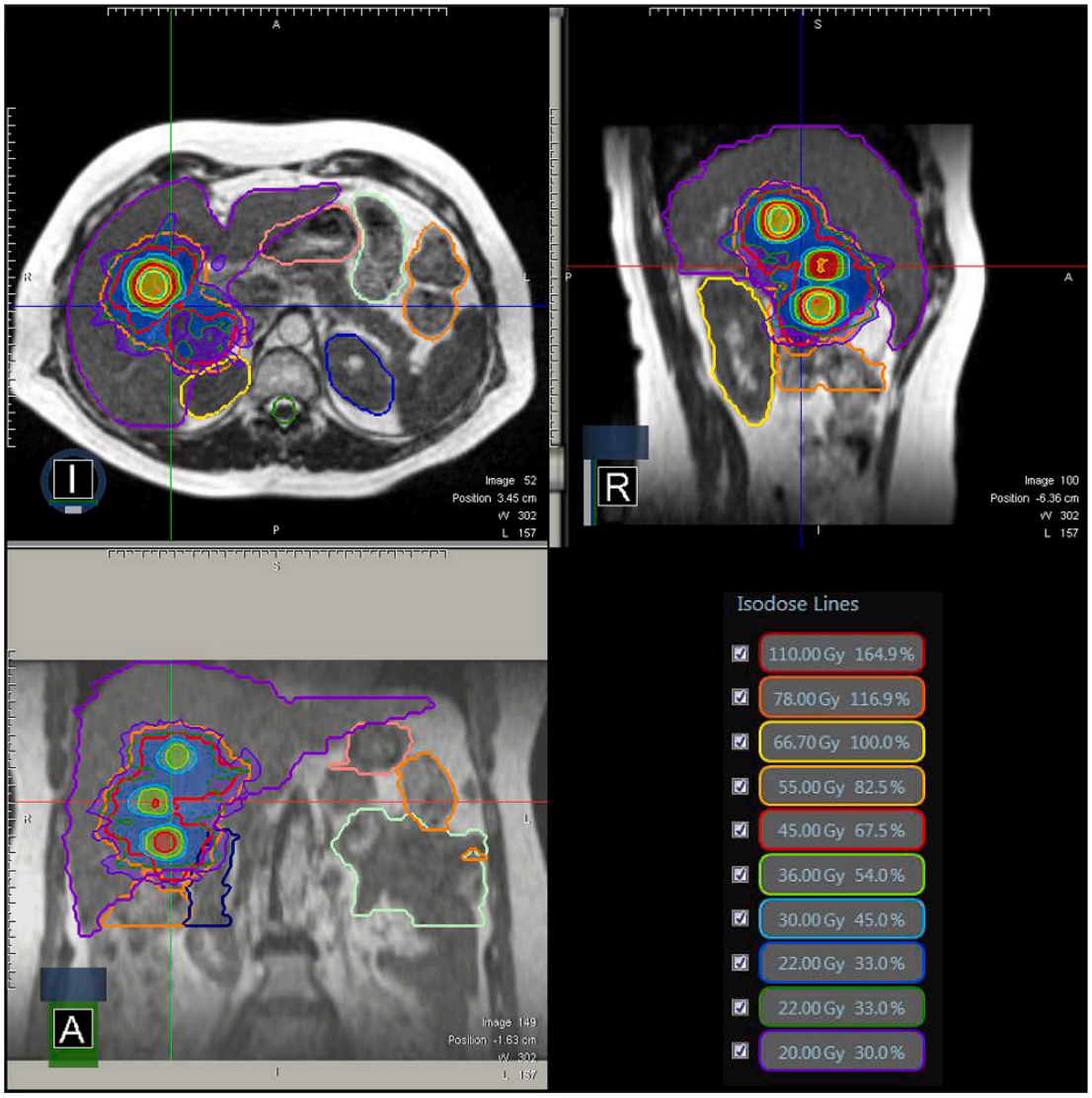

Fig. 1. Case 1 three plane isodoses. The target is located in the inferior portion of the bowel adjacent to the large bowel and duodenum.

Case 2

Presentation

A 55 year-old female initially presented with neck pain. A CT chest with contrast was obtained as a part of her work up which demonstrated multiple pulmonary nodules as well as multiple lesions of the left hemi-liver. A CT-guided biopsy of one of the liver lesions confirmed a diagnosis of metastatic IDH-1 mutated cholangiocarcinoma. She subsequently proceeded to progress through several cycles of chemo- and targeted systemic therapies over the next two years.

Most recently, she had been receiving Ivosidenib at a high-volume academic center. Her most recent surveillance CT chest/abdomen/pelvis demonstrated disease response in several bilateral pulmonary nodules, slight progression of several left hemi-liver masses which invaded the left hemi-diaphragm and gastric wall. The hepatic lesions were predominantly in segments two and three, and the largest of these was 4.7×4.3 cm. She was referred to radiation oncology for consideration of palliative radiotherapy. She denied abdominal pain although did note recent worsening of her gastroesophageal reflux disease. Her physical exam was notable for a tender abdomen at the right upper quadrant. She was recommended for Lattice SBRT for durable palliation of her hepatic metastases on a phase II clinical trial (NCI 0553471).

Quantitative analysis

A pseudo-arc deployment of 28 beams (11 deg of separation) and 88 segments was used in case 2. For planning, the relevant OARs were duodenum, large bowel, small bowel, esophagus, stomach, liver, and spinal cord. All OAR planning objectives were met. Coverage metrics included PTV_2000 V95%Rx = 99.4 % and PTV_6670 V95%Rx = 99.5 %. The dosimetric and spatially fractionated indices are reported in Table 2. Fig. 2 shows the isodose lines in three orthogonal planes intersecting the centroid of the GTV_2000. The average total gated beam delivery time was longer in case 2 at 36.9 min (range: 24.7 min – 50.5 min). The signal intensity changes relative to the PTV_Avoid ($R^2 = 0.01$) volumes over the course of treatment are minimal and are shown in Fig. 3.

Follow-up

At three months post-Lattice SBRT, the patient had surveillance imaging performed which demonstrated minimal interval partial response of treated lesions. The three month surveillance image was uploaded to the treatment planning software and the GTV was contoured, demonstrating a reduction in volume from 302.7 cc at time of simulation to 258.6 cc. At six months post-Lattice SBRT surveillance imaging demonstrated continued interval partial response of the radiated hepatic lesions as indicated by decreased size of the lesions. The

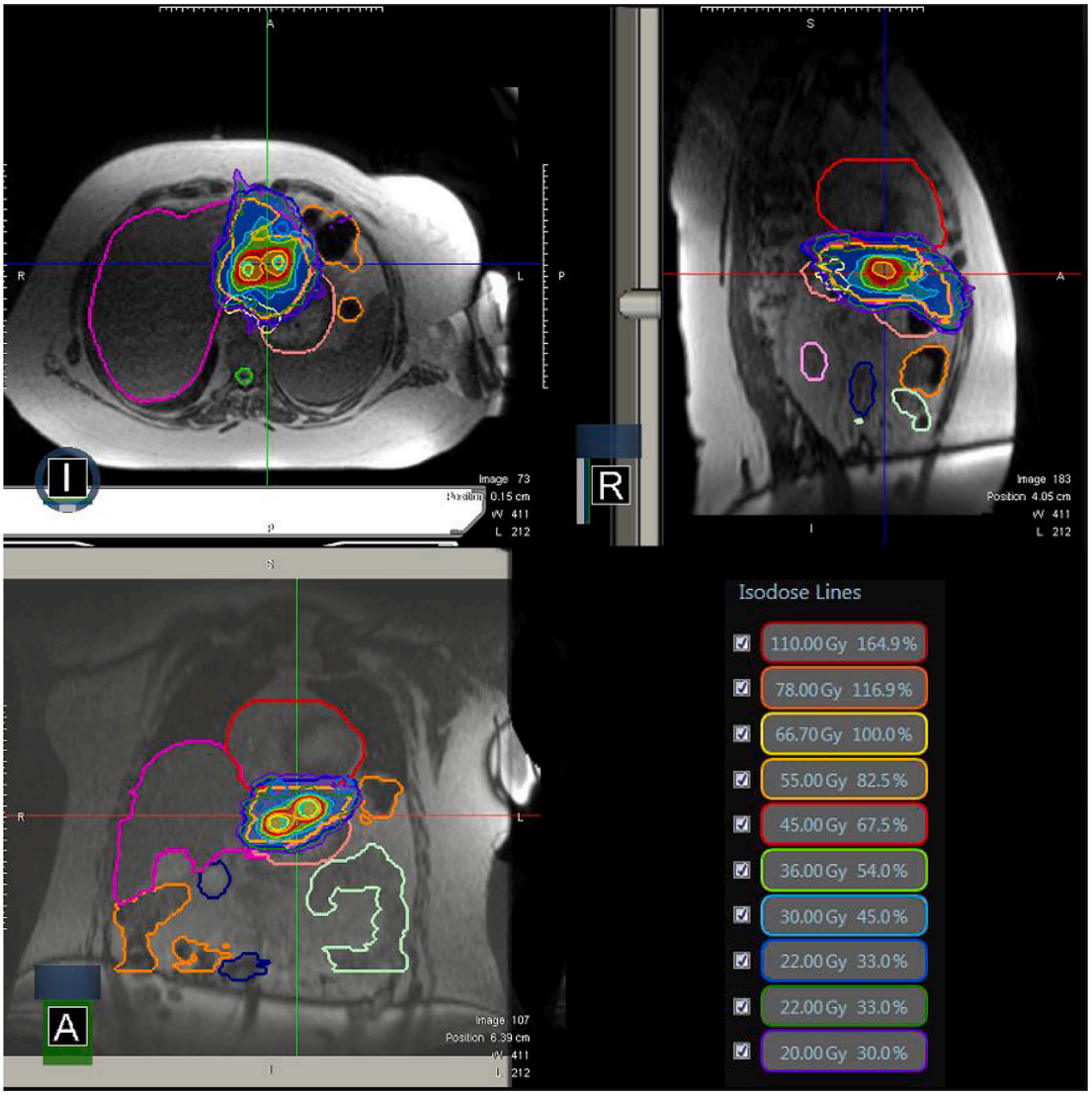

Fig. 2. Case 2 three plane isodoses. The target is located in the medial portion of the liver and is adjacent to the heart, stomach, and large bowel.

patient eventually progressed locally, regionally, and distantly, and remains alive on systemic therapy.

Discussion

This is one of the first reported use of MRgRT for lattice SBRT treatment. Abdominal treatment volumes in close proximity to OARs were successfully localized with improved precision compared to CBCT-guided treatment which can provide insufficient image quality to support abdominal treatments. Additionally, alignment and motion management was performed without the placement of fiducial markers. This eliminated the need for an invasive procedure to proceed with conventional linac treatment. Gated delivery was performed with real-time cine MRI which enabled reduced treatment volumes. For delivery, isocenter placement limitations due to scanner bore size and required use of a 6MV flattening filter free beam did not detract from similar plan quality metrics seen in other contemporary spatially fractionated studies [4,11].

For case 1, there was observed signal intensity changes in the high dose spheres over the course of treatment that is being investigated in subsequent patients. Longitudinal MRI acquired during MRI-linac adaptive therapy have high inter-fractional temporal resolutions and can potentially reveal unprecedented information about inter-fractional radiation-induced biological changes in tumor and normal tissues, especially under the increasingly popular hypo-fractionated RT treatment scheme. Although the exact mechanisms associated with SBRT and SFRT are still among the most intriguing and on-going active research topics, several early translational studies on animal models have clearly demonstrated that vascular-mediated indirect cell death can occur several hours or a few days after SBRT/SRS treatment[12]. Several pathophysiological events associated with indirect cell death related, such as cell swelling and tissue perfusion, could contribute to the observed inter-fractional MRI intensity changes in patients with lattice SBRT treatment. Consistently, several preliminary studies have recently demonstrated the feasibility of integrating radiomic parameters from daily inter-fractional MRI for tumor response evaluation of patients who underwent SBRT treatment of pancreatic cancer[13,14] and rectal cancer[15] on ViewRay MR-linacs. However, the prognostic significance of radiomics following treatment and the importance of signal changes observed in this study remains unclear.

MR-guided Lattice SBRT provides a treatment option for patients with abdominal disease without the need for an invasive fiducial marker placement or uncertainty during image alignment due to poor image quality.

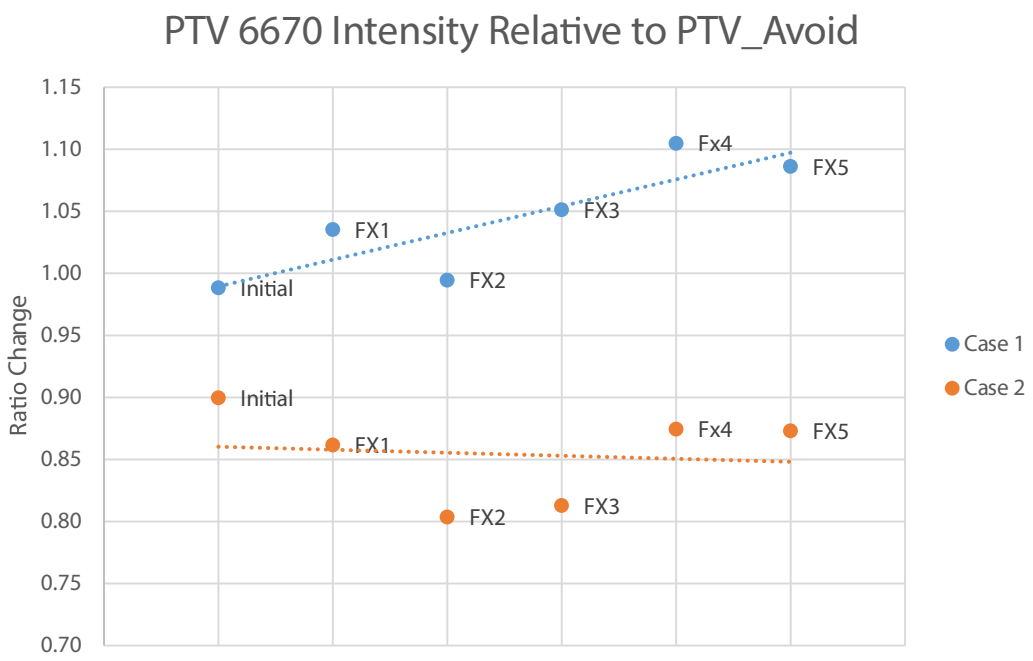

Fig. 3. Signal intensity changes in the PTV_6670 vol relative to the PTV_Avoid volumes over the course of treatment.

Declaration of Competing Interest

The authors declare that they have no known competing financial interests or personal relationships that could have appeared to influence the work reported in this paper.

Conflict of Interest Statement:

Drs. Green and Henke report honoraria, consulting fees and are on a ViewRay, Inc. medical advisory board.

Dr. Kim reports honoraria and grants from ViewRay, Inc.

Mr. Price reports honoraria from ViewRay, Inc.

None of the work presented in the case reported is related to the above mentioned CoIs.

Washington University in St. Louis has a master research agreement with ViewRay.

References

[1] Billena C, Khan AJ. A Current Review of Spatial Fractionation: Back to the Future? Int J Radiat Oncol 2019;104(1):177–87. https://doi.org/10.1016/J.IJROBP.2019.01.073.

[2] Mayr NA, Snider JW, Regine WF, Mohiuddin M, Hippe DS, Peñagarícano J, et al. An international consensus on the design of prospective clinical-translational trials in spatially fractionated radiation therapy. *Adv.* Radiat Oncol 2022;7(2). https://doi.org/10.1016/j.adro.2021.100866.

[3] Mohiuddin M, Miller T, Ronjon P, Malik U. Spatially Fractionated Grid Radiation (SFGRT): A Novel Approach in the Management of Recurrent and Unresectable Soft Tissue Sarcoma. Int J Radiat Oncol 2009;75(3):S526. https://doi.org/10.1016/J.IJROBP.2009.07.1200.

[4] Duriseti S, Kavanaugh J, Goddu S, Price A, Knutson N, Reynoso F, et al. Spatially fractionated stereotactic body radiotherapy (Lattice SBRT) for large tumors. *Adv Radiat Oncol* Published online 2021. https://doi.org/10.1016/j.adro.2020.100639.

[5] Noel CE, Parikh PJ, Spencer CR, Green OL, Hu Y, Mutic S, et al. Comparison of onboard low-field magnetic resonance imaging versus onboard computed tomography for anatomy visualization in radiotherapy. *Acta Oncol (Madr)* Published online 2015;54(9):1474–82.

[6] van Sörnsen de Koste JR, Palacios MA, Bruynzeel AME, Slotman BJ, Senan S, Lagerwaard FJ. MR-guided Gated Stereotactic Radiation Therapy Delivery for Lung, Adrenal, and Pancreatic Tumors: A Geometric Analysis. Int J Radiat Oncol Biol Phys 2018;102(4):858–66.

[7] Green OL, Rankine LJ, Cai B, Curcuru A, Kashani R, Rodriguez V, et al. First clinical implementation of real-time, real anatomy tracking and radiation beam control. Med Phys 2018;45(8):3728–40. https://doi.org/10.1002/mp.13002.

[8] Lamb JM, Ginn JS, O'Connell DP, Agazaryan N, Cao M, Thomas DH, et al. Dosimetric validation of a magnetic resonance image gated radiotherapy system using a motion phantom and radiochromic film. J Appl Clin Med Phys 2017;18(3):163–9. https://doi.org/10.1002/acm2.12088.

[9] Chuong MD, Bryant JM, Herrera R, McCulloch J, Contreras J, Kotecha R, et al. Dose-escalated magnetic resonance image-guided abdominoplevic reirradiation with continuous intrafraction visualization, soft tissue tracking, and automatic beam gating. *Adv.* Radiat Oncol 2022;7(2). https://doi.org/10.1016/j.adro.2021.100840.

[10] Ehrbar S, Käser SB, Chamberlain M, Krayebühl J, Wilke L, Mayinger M, et al. MR-guided beam gating: residual motion, gating efficiency and dose reconstruction for stereotactic treatments of the liver and lung. Radiother Oncol 2022;174:101–8. https://doi.org/10.1016/j.radonc.2022.07.007.

[11] Kavanaugh JA, Spraker MB, Duriseti S, Basarabescu F, Price A, Goddu M, et al. LITE SABR M1: Planning design and dosimetric endpoints for a phase I trial of lattice SBRT. Radiother Oncol 2022;167:172–8. https://doi.org/10.1016/J.RADONC.2021.12.003.

[12] Song CW, Glatstein E, Marks LB, Emami B, Grimm J, Sperduto PW, et al. Biological Principles of Stereotactic Body Radiation Therapy (SBRT) and Stereotactic Radiation Surgery (SRS): Indirect Cell Death. Int J Radiat Oncol Biol Phys 2021;110(1):21–34.

[13] Boldrini L, Cusumano D, Chiloiro G, Casà C, Masciocchi C, Lenkowicz J, et al. Delta radiomics for rectal cancer response prediction with hybrid 0.35 T magnetic resonance-guided radiotherapy (MRgRT): a hypothesis-generating study for an innovative personalized medicine approach. Radiol Med 2019 Feb;124(2):145–53. https://doi.org/10.1007/s11547-018-0951-y. Epub 2018 Oct 29. PMID: 30374650; PMCID: PMC6373341.

[14] Simpson G, Spieler B, Dogan N, Portelance L, Mellon EA, Kwon D, et al. Predictive value of 0.35 T magnetic resonance imaging radiomic features in stereotactic ablative body radiotherapy of pancreatic cancer: A pilot study. Med Phys 2020 Aug;47(8):3682–90. https://doi.org/10.1002/mp.14200. Epub 2020 May 16. PMID: 32329904.

[15] Cusumano D, Boldrini L, Yadav P, Casà C, Lee SL, Romano A, et al. Delta Radiomics Analysis for Local Control Prediction in Pancreatic Cancer Patients Treated Using Magnetic Resonance Guided Radiotherapy. Diagnostics (Basel) 2021 Jan 5;11(1):72. https://doi.org/10.3390/diagnostics11010072.